



Using UAV Imagery for Crop Analytics

Austin Coates, Casey Adams

Harris Geospatial Solutions, Inc. Broomfield, CO

**A Paper from the Proceedings of the
14th International Conference on Precision Agriculture
June 24 – June 27, 2018
Montreal, Quebec, Canada**

Abstract. *UAV imagery was collected in April and July of 2017 over a grape vineyard in California's San Joaquin Valley. Using spectral signatures, a landcover classification was performed to isolate table grapes from the background vegetation and soil. A novel vegetation index was developed based off the unique spectral characteristics of the yellowing effects of chlorosis within the table grape vines. Spatial statistics were run only on the pixels containing grape plants, and a relative vegetation health map was produced, using both the novel vegetation index and NDVI. Several regions within the map were identified as areas of interest and marked for further analysis. Automated temporal analysis showed that these areas of interest were in fact underperforming throughout the growing season. Field measurements later confirmed that these areas were suffering from a potassium deficiency. It was also shown that using a simple vegetation index, like NDVI, alone could not locate these anomalous areas even though it was present and measurable within the data.*

Keywords. *Remote Sensing, Multispectral, MicaSense, Spectral, ENVI, Multi-Temporal, Anomaly, Grapes, Vineyard, UAV, Drone, UAS, Hotspot, Spatial.*

The authors are solely responsible for the content of this paper, which is not a refereed publication.. Citation of this work should state that it is from the Proceedings of the 14th International Conference on Precision Agriculture. EXAMPLE: Lastname, A. B. & Coauthor, C. D. (2018). Title of paper. In Proceedings of the 14th International Conference on Precision Agriculture (unpaginated, online). Monticello, IL: International Society of Precision Agriculture.

Introduction

Remote sensing of vegetation can be a frustrating endeavor given that subtle nuances in spectral responses can signal dramatic changes in vegetation health and photosynthetic efficacy. This frustration is amplified when common remote sensing techniques, such as the tried and true Normalized Difference Vegetation Index (NDVI), fail to provide the required data and/or validations of the observed phenomena. It is for this reason that a deeper dive into the science of remote sensing is required to begin isolating and identifying these more subtle phenomena.

Taking this study as an example: early on, a field scout identified several plants within the test area that were showing signs of stress, visibly presenting itself through a yellowing of the leaves. The shift in visible pigmentation was quite possibly a result of a loss of chlorophyll. When chlorophyll and carotene are both present within a leaf, the leaf will reflect more green light (as compared to red and blue), thus appearing as green to the eye. However, when chlorophyll levels begin to dissipate, during senescence for example, red and green reflectance increases and the leaf begins to appear yellow in color (Sims & Gamon, 2002). In addition to the increase in red and green reflectance, the red edge (the sharp change in reflection at 710-720nm) can begin moving towards shorter wavelengths accompanied by a contraction in the chlorophyll absorption peak (Jones & Vaughan, 2010). However, depending on the level of senescence, the ratio between the red and near infrared reflectance can remain somewhat invariant. This ratio is the basis for NDVI (Rouse Jr, Haas, Schell, & Deering, 1974) so even with the apparent visual shift, NDVI may not register the stress until it is too late.

The intent of the paper is to show the reader potential vegetation monitoring solutions beyond NDVI. This study is not meant to be an exhaustive analysis of a specific phenomenon but rather an introduction to topics and hopefully a stepping off point for many.



Figure 1: Healthy (left) and stressed (right) vines, as seen from in-field inspection (Micasense, 2017a).

Methods

Study Area

The study site is located in the California's San Joaquin Valley. This region has a population of roughly 4 million people and is one of the most productive agricultural regions in the world (Environmental Protection Agency, 2018). The imagery was collected over Brandt Farms and the target vegetation type in this scene is table grapes. Two images were collected over the site, one on April 26, 2017 and one later in the season on July 10, 2017. In the April image, there was considerable ground cover vegetation between rows and the target vegetation had yet to achieve

full canopy closure, whereas in the July image, some of the groundcover vegetation has been removed and full canopy closure has been achieved.

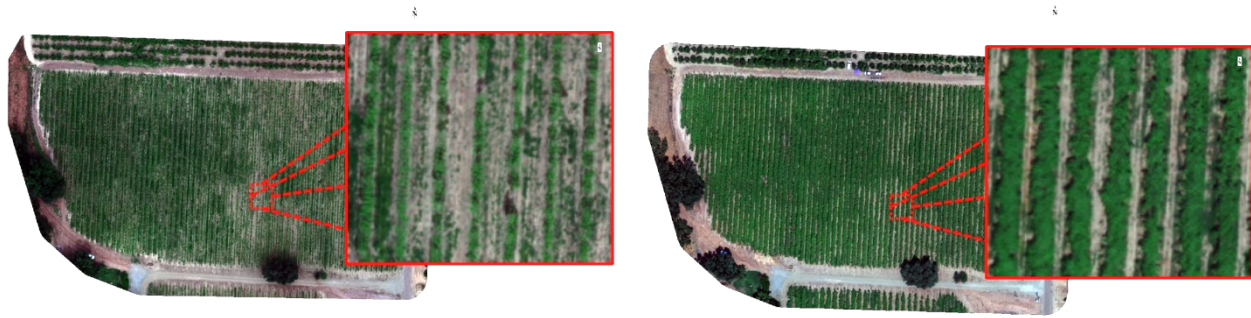


Figure 2: Orthomosaic of Brandt Farms. Image on the left was captured early in the season (4/26/2017) before full canopy closure. Image on the right is later in the season (7/10/2017) after canopy closure.

Image Data

The imaging platform used in this study was a 3DR Solo (e.g. unmanned aerial vehicle). This platform was used because it is inexpensive and could comfortably carry the weight of the imager. A MicaSense RedEdge camera was used to capture the imagery. The MicaSense RedEdge acquired five narrow, spectral bands simultaneously which were saved to an onboard SD card. The RedEdge camera has five spectral bands running from visible through near infrared.

Images were also taken of a Calibrated Reflectance Panel (CRP) which were provided by MicaSense. The CRP provided us with a reference point from which reflectance values could be derived.

Preprocessing

A grid pattern was flown over the study area which provided adequate forward and side overlap for later orthomosaic generation. The raw imagery was initially captured by the MicaSense RedEdge sensor then analyzed using PrecisionPass (Harris Geospatial Solutions Inc., 2018d). The camera parameters, side lap, forward overlap, image saturation, and image contrast were deemed appropriate and a decision was made to leave the study area without flying again. Before orthorectification and mosaicking could be performed, the imagery was stacked and converted to reflectance values. The imagery was co-aligned and stacked using the UAV Toolkit (Norman & Harris Geospatial Solutions Inc., 2018) and the conversion from radiance to reflectance was done using Equation 1 (MicaSense, 2017b).

$$F_i = \frac{\rho_i}{avg(L_i)}$$

Equation 1: Conversion from radiance to reflectance calibration factor. Where F_i is the reflectance calibration factor for band i , ρ_i is the average reflectance of the CRP for the i th band, and $avg(L_i)$ is the average value of the radiance for the pixels inside the panel for band i .

Once the reflectance image stacks were created, they were orthorectified and mosaicked using ENVI OneButton (Icaros, 2017).

Analysis

In order to do all of the image processing and analysis, it was imperative that a remote sensing-specific software suite was used. We decided to use ENVI + IDL and the ENVI Crop Science module for these tasks (Harris Geospatial Solutions Inc., 2018a, 2018b) because of its ease of use and large breadth of tools available. To begin, we first isolated the target vegetation (i.e. table

grapes) from the ground cover. This was an important step because later in the workflow, multiple global and local statistics were run, and by including background pixels, it raises the risk of skewing the resulting statistics due to the effects of spatial autocorrelation. Spatial autocorrelation occurs when the presence of a specific material or characteristic affects the presence of the same material or characteristic simply through the collocation with another material (Congalton & Green, 2008). By isolating the target vegetation, we could compare like materials to one another to isolate subtle variations in spectral characteristics.

To segment and classify the images, a spectral library was automatically built using Spectral Maximum Angle Convex Cone (SMACC) (Gruninger, Ratkowski, & Hoke, 2004). This algorithm looks for an abundance of spectral endmembers and then creates a spectral library of these endmembers. Since the images are primarily made up of ground cover vegetation, table grapes,

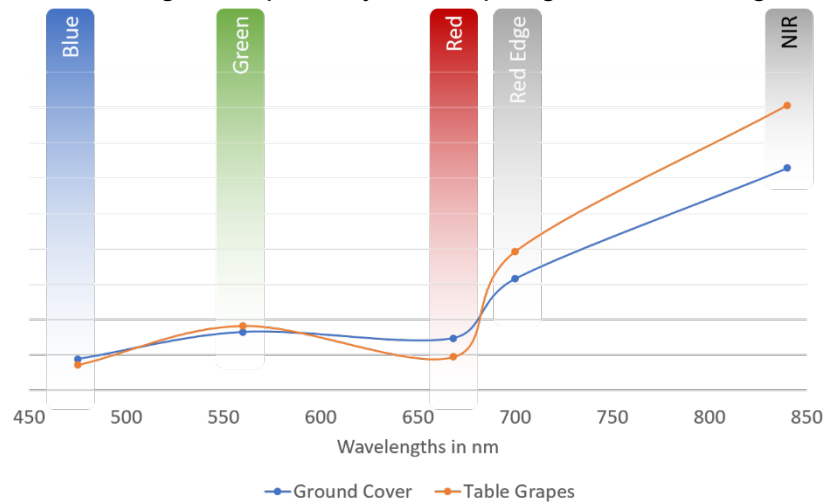


Figure 3: Ground cover and table grape spectra

and soil, the algorithm was able to successfully separate the spectra of the table grapes from all other spectral profiles (Figure 3). Once the spectral library was built, spectral angle mapper (SAM) was used to classify the image because it is relatively insensitive to illumination and albedo effects. Variations in illumination intensity were present within the collections because this dataset was collected in small sections and reconstructed into one large image. SAM mitigates illumination effects by creating a vector for each spectra in the spectral library and mapping it into multidimensional space (e.g. the number of dimensions are equal to the number of bands). The angle of each target spectra vector is compared with that of each pixel's vector within the image. If the angle of a pixel in the image falls within x user-defined degrees of one of the target spectra's then it is classified as that target spectra (Kruse et al., 1993).

Once the target vegetation was isolated, manual spectral analysis was performed by examining the spectra at the locations where yellowing was observed. This revealed that the stressed vegetation had higher reflectance values in the blue, green, red, and red edge bands as compared to healthy green vegetation. There was also a lower spectral reflectance observed in the near infrared band, as compared to healthy green vegetation. To take advantage of these observations, a novel vegetation index was derived.

$$\frac{\rho_{NIR} - \rho_{Red\ Edge}}{\rho_{Green} - \rho_{Red} - \rho_{Blue}}$$

Equation 2: Novel vegetation index designed to take advantage of the unique bands available from the MicaSense RedEdge sensor. ρ_{Blue} = 475nm, ρ_{Green} = 560nm, ρ_{Red} = 668, $\rho_{Red\ Edge}$ = 717nm, ρ_{NIR} = 840nm

This index captures the difference between the location of the red edge absorption feature and that of the near infrared, while also using the ratio between the visible and non-visible portions of the spectra. This vegetation index was based off of the proven efficacy of the Simple Ratio (SR)

vegetation index (Birth & McVey, 1968).

To track the changes occurring over the growing season, a trend analysis was performed. The “find developing hotspots” tool created by Harris Geospatial Solutions, Inc. was used for this purpose. This tool creates a trendline for the study area and then analyzes deviations from that trend. This tool also uses spatial statistics to define regions that are statistically significant, then computes the level of significance as compared to the rest of the regions under review. By combining the trend analysis and spatial statistics, the resulting data layers shows regions within a field that are statistically significant with respect to spatial information in addition to statistically significant in terms of developmental trends (Harris Geospatial Solutions Inc., 2018c).

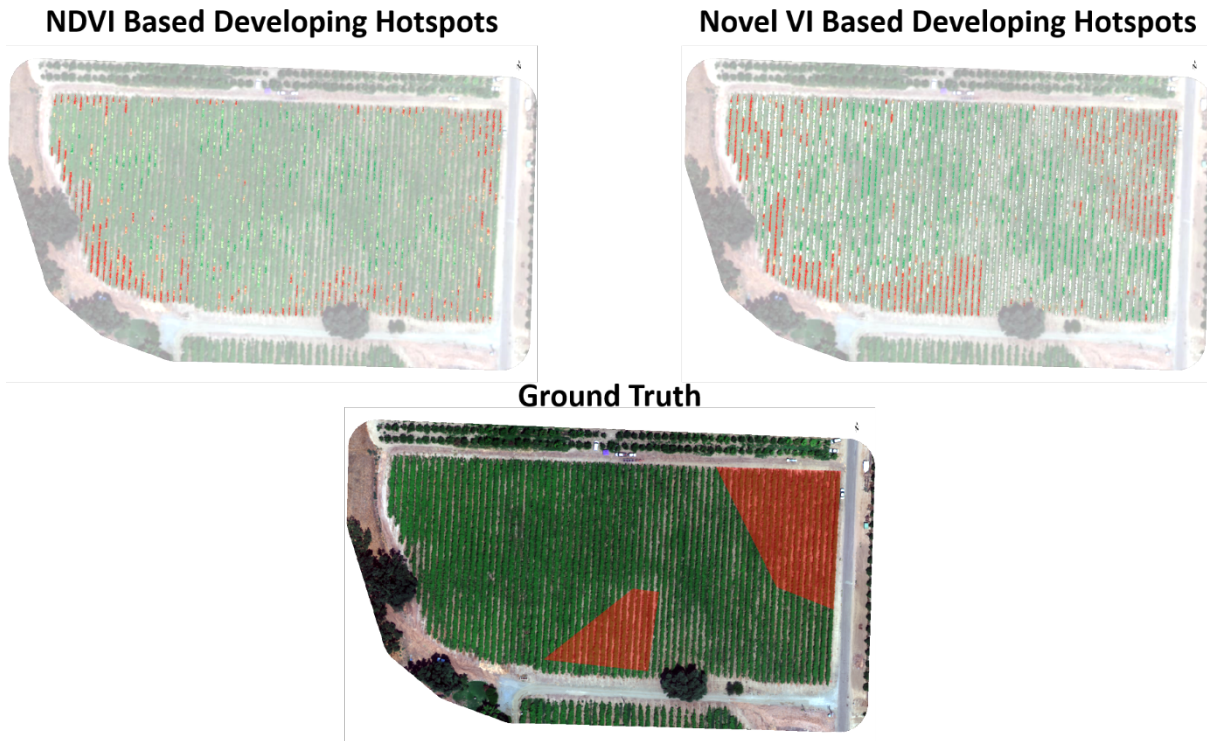


Figure 4: Developing Hotspots resulting images. Red areas, in the developing hotspot images, indicate regions that are statistically significant and are trending well below the mean level of the field. Red area in the ground truth image shows the yellowing regions identified by the field scout.

Results and Discussion

Using the novel vegetation index discussed above, we have been able to more accurately identify and map areas within the field that have been affected. Tissue tests revealed that the yellowing seen early on was the effect of low levels of potassium. Variations in nutrient uptake can manifest themselves in many ways. In this case, a lack of potassium lead to chlorosis (a low level of chlorophyll in the leaves). Chlorosis can cause leaf die off which may result in fruit sunburn, variations in color uniformity, and issues associated with bunch/berry size.

By comparing the red regions in the NDVI image to those in the novel vegetation index in Figure 4, it is clear that considering the full spectral profile of the phenomena, we are able to derive more

information and identify costly problems much earlier. Luckily this issue was quickly mapped and remediation efforts can now be undertaken for next year.

NDVI is an incredibly useful algorithm; however, in some cases, it is not finely tuned enough to see actionable results. While it is not always necessary to have a custom index built for each phenomenon, it is important to consider what physiological forces are at play and how they can be measured. By knowing the way in which light interacts with the vegetation in question, it was possible to narrow in on an equation that leveraged the power of the sensor being used as well as the physical characteristics being mapped.

Conclusions

Much of the literature that deals with vegetation uses NDVI as a starting point and then expands from there after results are not sufficient. However, we can see that it is often better to first look at the characteristics of the target that is being mapped and identify unique features associated with that material (e.g. yellowing leaves, wilting leaves, loss in moisture concentration...). Once these key features have been identified, then one can look at how this is being manifested in the spectra. Then, and only then, should the decision be made to deploy a tried and true vegetation index like NDVI.

Acknowledgements

Thank you to MicaSense and Chris Thiesen for providing the imagery and supporting documentation and our sincere appreciation goes to Brandt Farms for allowing us to study one of their vineyards.

References

- Birth, G. S., & McVey, G. R. (1968). Measuring the Color of Growing Turf with a Reflectance Spectrophotometer 1. *Agronomy journal*, 60(6), 640-643.
- Congalton, R. G., & Green, K. (2008). *Assessing the accuracy of remotely sensed data: principles and practices*. CRC press.
- Environmental Protection Agency. (2018, 4/3/2018). San Joaquin Valley. Retrieved from <https://www.epa.gov/sanjoaquinvalley>
- Gruninger, J. H., Ratkowski, A. J., & Hoke, M. L. (2004). *The sequential maximum angle convex cone (SMACC) endmember model*. Paper presented at the Algorithms and technologies for multispectral, hyperspectral, and ultraspectral imagery X.
- Harris Geospatial Solutions Inc. (2018a). ENVI + IDL (Version 5.5). Broomfield, CO: Harris Geospatial Solutions Inc.
- Harris Geospatial Solutions Inc. (2018b). ENVI Crop Science (Version 1.1). Broomfield, CO: Harris Geospatial Solutions Inc.
- Harris Geospatial Solutions Inc. (2018c). Find Developing Hotspots. *Docs Center*. Retrieved from <https://www.harrisgeospatial.com/docs/FindDevelopingHotspots.html>
- Harris Geospatial Solutions Inc. (2018d). PrecisionPass (Version 1.0). Broomfield, CO.
- Icaros. (2017). ENVI OneButton Professional Edition (Version 5.1.0.57).
- Jones, H. G., & Vaughan, R. A. (2010). *Remote sensing of vegetation: principles, techniques, and applications*. Oxford university press.
- Kruse, F. A., Lefkoff, A., Boardman, J., Heidebrecht, K., Shapiro, A., Barloon, P., & Goetz, A. (1993). The spectral image processing system (SIPS)—interactive visualization and analysis of imaging spectrometer data. *Remote Sensing of Environment*, 44(2-3), 145-163.
- Micasense. (2017, 3/3/2017a) Mapping Table Grapes in the San Joaquin Valley. Retrieved from <https://blog.micasense.com/mapping-potassium-deficiency-table-grapes-in-the-san-joaquin-valley-434a4b85a80e>

- MicaSense. (2017, 7/24/2017b). Use of Calibrated Reflectance Panels For RedEdge Data. *Processing Data*. Retrieved from <https://support.micasense.com/hc/en-us/articles/115000765514-Use-of-Calibrated-Reflectance-Panels-For-RedEdge-Data>
- Norman, Z., & Harris Geospatial Solutions Inc. (2018). UAV Toolkit (Version 2.1). Broomfield, CO: Harris Geospatial Solutions Inc.,. Retrieved from <https://github.com/envi-idl/UAVToolkit>
- Rouse Jr, J. W., Haas, R., Schell, J., & Deering, D. (1974). Monitoring vegetation systems in the Great Plains with ERTS.
- Sims, D. A., & Gamon, J. A. (2002). Relationships between leaf pigment content and spectral reflectance across a wide range of species, leaf structures and developmental stages. *Remote Sensing of Environment*, 81(2-3), 337-354.